ARTICLE NO. 79-0060R

C 80-015

Evaluation of a Describing Function Approach to Nonlinear Gust Loads Analysis

00016
00027
00029

Robert L. Stapleford* and Richard J. DiMarco†
Systems Technology, Inc., Hawthorne, Calif.

Structural loads on the vertical tail of an aircraft with a limited authority yaw damper are calculated. The results of a random input describing function analysis are compared with those of a Monte Carlo simulation. Comparisons of exceedance rates and other statistics are presented. The mission analysis criterion for continuous turbulence is used to establish the design limit load. The describing function analysis consistently underestimates the design limit load for two different authority limits. The cause of this discrepancy is examined, and a simplified procedure is developed to assess the necessity for, and adequacy of, describing function analyses.

Nomenclature

F_t = aerodynamic force on tail
F_β, F_δ = derivatives of F_t with respect to sideslip and rudder deflection
I_z = aircraft yaw moment of inertia
K_R = yaw damper gain
l_t = distance from aircraft c.g. to c.p. of tail
m = aircraft mass
r = yaw rate
s = Laplace transform operator
v = lateral inertial velocity
v_g = lateral gust velocity
V = true airspeed
β = c.g. sideslip angle (v/V)
β_t = tail sideslip angle
δ_R = rudder deflection
$\delta_{R_{\text{limit}}}$ = rudder authority limit
σ_{v_g} = root mean square of lateral gust velocity
τ = time constant for aerodynamic lag in force buildup
ϕ_{v_g} = power spectral density of v_g
ω = angular frequency
ω_g = break frequency of ϕ_{v_g}

Parameter Values

V = 750 ft/s
m = 20,000 slugs
I_z = 5.2449×10^7 slug-ft^2
l_t = 102.42 ft
F_β = -5.0853×10^5 lb/rad
F_δ = 2.5605×10^5 s^{-2}
K_R = 1.0 s
τ = 0.1 s
$\delta_{R_{\text{limit}}}$ = 3.6 deg (nominal)
ω_g = 0.42857 rad/s

Introduction

INCREASING emphasis is being placed on the effects of continuous random turbulence on aircraft structural and control systems design. Recently,[1] specific criteria for continuous gust loads on large aircraft have been proposed for inclusion in Federal Aviation Regulations (FAR) Part 25. This proposal offers the designer a choice of using either design envelope analysis or mission analysis in combination with supplementary design envelope analysis to establish design limit loads. These requirements largely reflect the current state of the art in this area, and their addition should be a significant step in improving aircraft structural design. However, there are a number of potential problems and difficulties in applying the proposed criteria.

One of the most prominent problems is how to include the effects of system nonlinearities in the required gust loads analyses. Significant nonlinearities can come from several sources, including the basic aerodynamic characteristics of the aircraft and various rate/position limits in the flight control system. The proposed design criteria rely on power spectral analysis techniques to quantify key criteria parameters. These techniques cannot be directly applied to a nonlinear system. Some other more complex and more costly procedure must be used.

One obvious alternative is to conduct a time domain simulation using an exact model of the nonlinear system. The desired criteria parameters could then be obtained to any desired accuracy by making the runs sufficiently long. The cost of such a simulation, however, could easily be prohibitive. Very long runs are required to get reliable data for the very low exceedance rates associated with design loads. Moreover, a large number of runs might be required to cover the necessary combinations of weight, c.g., speed, altitude, rms gust levels, etc.

A time domain simulation approach was taken in the design of the L-1011 yaw damper.[2] Cost in that case was minimized by using an existing simulation and making relatively short (600 s) runs at only the most critical combination of conditions. The loss of accuracy due to these approximations was compensated for by interpreting the results conservatively.

This selective simulation approach is obviously not as costly as a full blown Monte Carlo simulation. However, it may not always be easy to make a conservative yet cost effective estimate of design loads from such limited results. Moreover, an analytical solution might provide an even more substantial cost benefit.

One such approach is to use random input describing function analysis—a technique commonly used in servo analysis work—to approximate the nonlinearity as an effective gain. Linear analysis techniques can then be applied to the approximate model. Such an approach has previously been developed for the analysis of nonlinear systems with the amplitude modulated random process (Press model) for atmospheric turbulence.[3]

Received Dec. 14, 1978; presented as Paper 79-0060 at the AIAA 17th Aerospace Sciences Meeting, New Orleans, La., Jan. 15-17, 1979; revision received June 11, 1979.

Index categories: Structural Design (including Loads); Simulation; Guidance and Control.

*Principal Research Engineer. Associate Fellow AIAA.
†Staff Engineer, Research.

The application of the random input describing function technique is further investigated here. A simple example will be used to demonstrate this approach to the determination of design limit load based on the mission analysis criteria. First, the design limit load will be determined by describing function analysis. Then a corresponding result will be obtained from a time domain simulation. Comparison of these results leads to the development of a simple procedure for assessing the necessity for, and the adequacy of, describing function analysis in the general case.

The example analysis is summarized herein. Essential technical details are provided in the Appendix. More complete documentation of this analysis is available elsewhere.[4]

Problem Definition

Mission Analysis Criteria

In the mission analysis scheme proposed in FAR Part 25, the expected aircraft utilization is divided into a number of mission segments. For each segment, power-spectral techniques are used to compute values of $\bar{A}$, the ratio of rms incremental load to rms gust velocity, and N_0, the rate of upward axis crossings. These quantities are then used to compute exceedance rates as a function of load level, according to:

$$N(\Delta x) = \sum_i \tau_i N_0 \left[P_1 \exp\left(-\frac{|\Delta x|}{b_1 \bar{A}} \right) + P_2 \exp\left(-\frac{|\Delta x|}{b_2 \bar{A}} \right) \right] \quad (1)$$

where

τ_i = fraction of time in the ith segment
Δx = net load or stress minus 1g flight value
P_1, P_2 = probabilities of encountering nonstorm and storm turbulence
b_1, b_2 = rms values of rms gust velocity for nonstorm and storm turbulence

The values of P_1, P_2, b_1, and b_2 are given as functions of altitude. The design limit loads are those for which the exceedance rate is 2×10^{-5}/h.

Equation (1) cannot be directly applied to nonlinear systems to obtain load exceedance rates. The immediate problem is that $\bar{A}$ and N_0 are no longer constant as they are for a linear system. More importantly, the aircraft response parameters are no longer normally distributed. To fully appreciate the extent of the problem one needs to understand the derivation of Eq. (1). This derivation is provided in the Appendix. The equations contained therein will also be used in the nonlinear analyses.

System Model

The problem selected for study is the analysis of the lateral tail loads for an aircraft with a limited-authority yaw damper. This is a useful example since the yaw damper can greatly reduce tail loads, and therefore damper limiting may have substantial effect. A 20% reduction in lateral gust design loads is attributed to the L-1011 yaw damper.[2,5] Such an effect is neither new nor uncommon among large jet aircraft. Increased lateral load levels due to yaw damper saturation in turbulence caused a serious problem for a first generation swept wing bomber in the early sixties.[6] Thus the example problem is both realistic and of practical concern.

The principal objective of this analysis is to determine the exceedance rates of limit level tail loads. It is at these load levels that the accuracy of a describing function analysis is of greatest concern. Accurate measurement of these very low rates in the time domain requires rather long time histories. To reduce the cost of these computations, the model used in the analysis was kept as simple as possible without sacrificing any of the essential elements of the yaw damper problem. A complete definition of this model is given in the Appendix. Its key features are:

1) Roll motion is ignored.
2) Only aerodynamic forces and moments due to the vertical tail are included.
3) Structural modes are not included.
4) Yaw damper used pure gain feedback of yaw rate.
5) Unsteady lift effects are approximated by first-order lag (this allows exact calculation of axis crossing rate for tail load).
6) Gust spectrum is modeled as white noise passed through first-order filter.

The resulting model has two degrees of freedom—side velocity and yaw rate—yielding equations of motion whose solution is only fourth order (including one for the gust filter). Model parameter values were selected to provide a good match to the dutch roll characteristics given for the 747 at 40,000 ft and Mach 0.8.[7] As is typical of large jet aircraft, the unaugmented 747 exhibits very low dutch roll damping at high speed and altitude. For the selected flight condition, the aircraft exhibits a damping ratio of 0.035 at a natural frequency of 1.0 rad/s. Closure of the yaw damper loop substantially increases the damping ratio of this mode to 0.292. This reduces rms tail loads by nearly two-thirds. Thus, a damper authority limit in this flight condition has a potentially large effect on tail loads.

Though inertial loads have not been explicitly included in this model, the total structural load is generally well approximated by the aerodynamic component. In this simple example, in fact, structural and aerodynamic loads are exactly proportional.

Describing Function Analysis

The imposition of a rudder limit can reduce the effectiveness of the yaw damper loop closure. Whenever the rudder deflection commanded by yaw rate exceeds the authority limit, the damper, in effect, operates at less than the full yaw-rate-to-rudder gain. The effect of this limiting over the course of time in turbulence can be linearized in terms of an "average" yaw-rate-to-rudder gain. When normalized by the actual system gain, this "effective gain" takes on a value between 1, corresponding to damper operation with no limit, and 0, corresponding to unaugmented operation. Within these limits, the value depends on the characteristics of the patch of turbulence traversed, the system response, and the authority limit.

One way of specifying the effective gain is the random input describing function.[8] The value of this function is chosen to minimize the variance of the difference between the outputs of the nonlinearity and its linear approximation. This value is a function of the probability density of the input to the nonlinearity. In the yaw damper example, this input, as well as all other response variables, is assumed to be a normally distributed random variable, like the lateral gust velocity σ_{v_g} which is the system input. Then, the describing function approach quantifies the effective gain as a function only of the damper authority and the rms level of the input to the nonlinearity. The details of this quantification are treated in the Appendix.

Calculation of Conditional Probabilities

Transfer functions for the limited-authority system can be calculated by closing the damper loop with the effective gain. From these "effective" transfer functions, values of $\bar{A}$ and N_0 for the load on the vertical tail can be calculated using standard power spectral analysis techniques. These values are functions of the σ_{v_g} corresponding to the effective gain, at the given authority limit.

The calculation procedure which was used can be summarized as follows:

1) Assume an effective yaw damper gain k_{DF}.
2) With this gain, compute various closed-loop transfer functions for a lateral gust input.

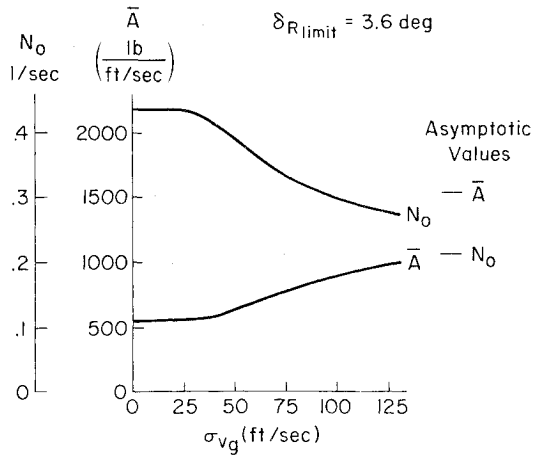

Fig. 1 Variations of describing function analysis parameters with gust velocity.

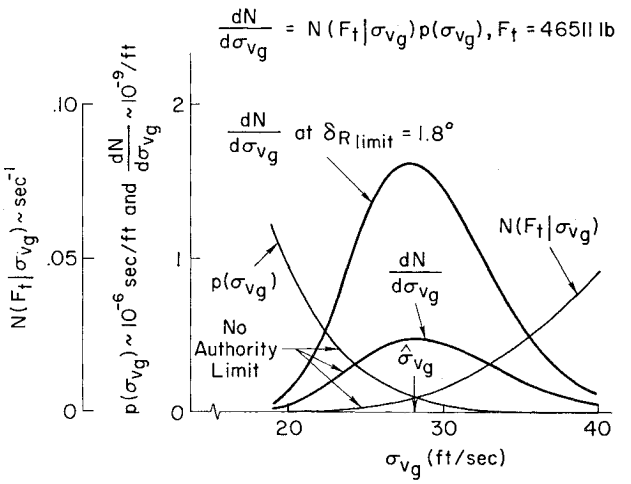

Fig. 2 Variations of exceedance rate integrand with gust velocity.

3) Compute N_0 and $\bar{A}$ for the tail load.

4) Compute the ratio, (rms input to limiter)/(rms gust velocity).

5) Use this ratio and the effective gain to compute those combinations of rms gust velocity and rudder authority limit which would produce that effective gain.

Figure 1 gives $\bar{A}$ and N_0 as a function of rms gust velocity for a rudder authority limit of 3.6 deg, which is approximately equivalent to the 747 limit. As Fig. 1 shows, for this rudder authority, it takes gust velocities somewhat greater than 25 ft/s rms to change the value of these two parameters substantially. On the other end of the scale, as the gust velocity increases, $\bar{A}$ and N_0 approach asymptotic values corresponding to unaugmented operation. These asymptotic values differ greatly from those for the unlimited yaw damper—by factors of, roughly, 3 and 0.5, respectively.

Based on the assumption that the tail load F_t is normally distributed, its exceedance rates for a given rms gust velocity are analytically defined as functions of $\bar{A}$ and N_0, just as for a linear system, by:

$$N(F_t|\sigma_g) = N_0 \exp[-\tfrac{1}{2}(F_t/A\sigma_{v_g})^2] \tag{2}$$

In this case, however, $\bar{A}$ and N_0 are functions of σ_{v_g}.

Overall Exceedance Rates

The final step in this analysis is to use these conditional exceedance rates to compute overall exceedance rates. This is done by numerically integrating the conditional tail load exceedance rates over the range of σ_{v_g}:

$$N(F_t) = \int_0^\infty N(F_t|\sigma_{v_g})p(\sigma_{v_g})\,d\sigma_{v_g} \tag{3}$$

For a full-scale mission analysis, this integration is done for each mission segment. Segment exceedance rates are then weighted by the corresponding τ_i and summed as in Eq. (1). For this example, the mission profile has been reduced to a single flight condition for simplicity.

The gust velocity distribution of interest in this case is the one implicitly specified in the mission analysis design criteria:

$$p(\sigma_{v_g}) = \sqrt{\frac{2}{\pi}}\left\{\frac{P_1}{b_1}\exp\left[-\frac{1}{2}\left(\frac{\sigma_{v_g}}{b_1}\right)^2\right] + \frac{P_2}{b_2}\exp\left[-\frac{1}{2}\left(\frac{\sigma_{v_g}}{b_2}\right)^2\right]\right\} \tag{4}$$

At the 40,000 ft altitude of the example, the FAR gust distribution parameters P_1, P_2, b_1, and b_2 take on the values 0.007, 0.00011, 3.0 ft/s, and 9.36 ft/s respectively. This completes the definition of the terms in Eq. (3).

Critical Gust Velocity

Before presenting the results of that integration, it is instructive to try to predict the outcome. Consider the case of no yaw damper limit. Overall exceedance rates for this linear system can be computed using Eq. (3), just as for the nonlinear case; of course, the computation is simpler since $\bar{A}$ and N_0 are constant. Figure 2 shows the variation of the integrand $dN/d\sigma_{v_g}$ and its component factors $N(F_t|\sigma_{v_g})$ and $p(\sigma_{v_g})$ with σ_{v_g}, for F_t = 46,511 lb. This value of tail load is the design limit load with no damper limit, based on the mission analysis design criteria of 2×10^{-5} exceedances per hour (5.56×10^{-9}/s).

Figure 2 shows that the integrand has a well-defined peak. Below the peak, the integrand drops rapidly because the decrease in the conditional exceedance rate for F_t quickly outpaces the increased probability of encountering the lower gust levels. Above the peak the decrease in gust intensity probability dominates.

The "critical" value of gust velocity at which $dN/d\sigma_{v_g}$ is maximum can be closely approximated analytically. The simplifying approximation is that over the range of interest,

$$p(\sigma_{v_g}) \doteq \sqrt{\frac{2}{\pi}}\frac{P_2}{b_2}e^{-(\frac{1}{2})(\sigma_{v_g}/b_2)^2} \tag{5}$$

i.e., that

$$\frac{P_1}{b_1}e^{-(\frac{1}{2})(\sigma_{v_g}/b_1)^2} \ll \frac{P_2}{b_2}e^{-(\frac{1}{2})(\sigma_{v_g}/b_2)^2} \tag{6}$$

Differentiating the linear system integrand with respect to σ_{v_g} with the nonstorm turbulence term omitted yields

$$\frac{d}{d\sigma_{v_g}}[N(F_t|\sigma_{v_g})p(\sigma_{v_g})] \doteq N(F_t|\sigma_{v_g})\left[\left(\frac{F_t}{\bar{A}}\right)^2\frac{1}{\sigma_{v_g}^3}\frac{1}{b_2^2}\sigma_{v_g}\right] \tag{7}$$

Thus the rms gust velocity which maximizes the integrand is given by

$$\hat{\sigma}_{v_g} \doteq (b_2F_t/\bar{A})^{\frac{1}{2}} \tag{8}$$

This gives a critical gust velocity of 28.2 ft/s for the peak shown in Fig. 2. This value lies close to the center of the in-

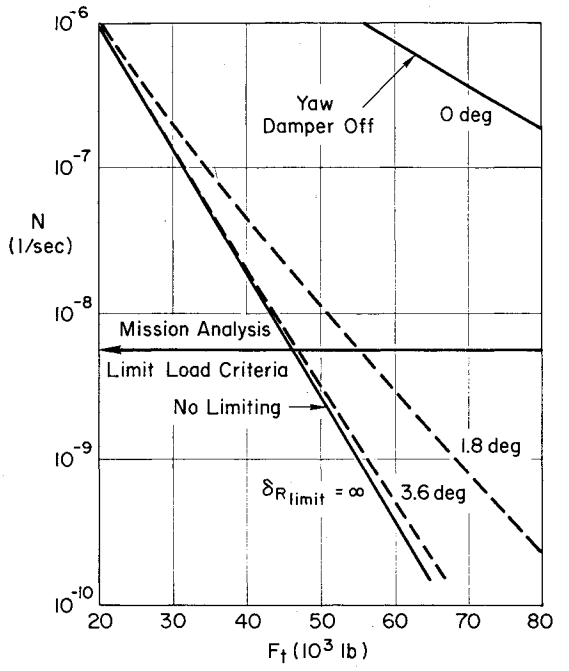

Fig. 3 Overall exceedance rates based on describing function analysis.

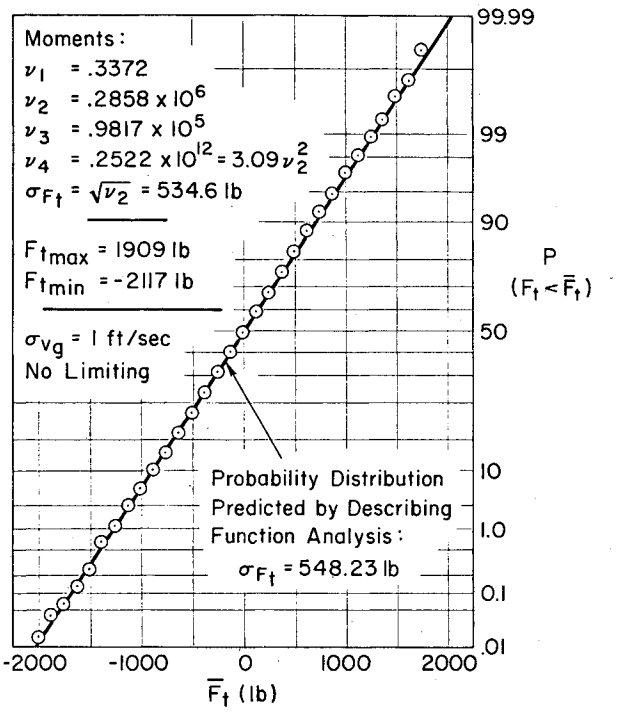

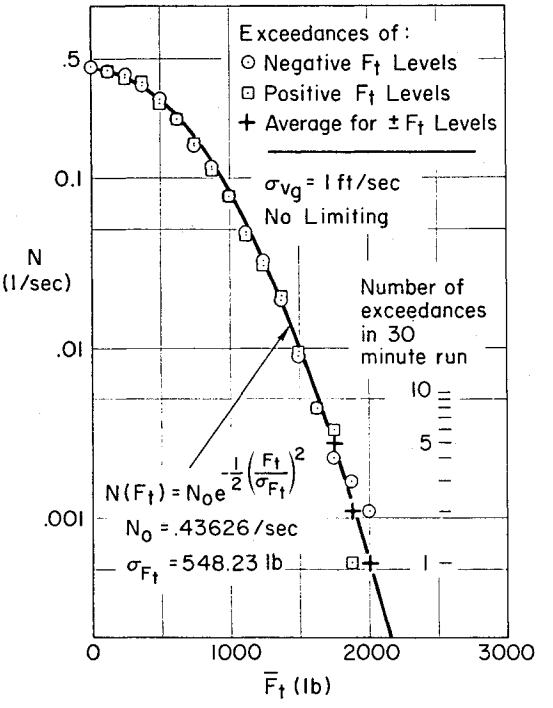

Fig. 4 Validation data for time domain simulation: a) Probability distribution for $k_{DF} = 1$; b) Exceedance rates for $k_{DF} = 1$.

terval from 20 ft/s to 40 ft/s for which the integrand has significant value.

The purpose of the above is to demonstrate that the critical gust range is easily predicted and is roughly 20-40 ft/s for this example. Gust levels outside this range do not contribute substantially to the design load overall exceedance rate.

In Fig. 1 it is seen that only as gust velocity approaches the high end of the 20-40 ft/s range do the values of $\bar{A}$ and N_0 begin to depart appreciably from their no-limit levels. At 40 ft/s rms, $\bar{A}$ has increased from 548 to 583 lb-s/ft and N_0 has decreased from 0.436 to 0.414 s^{-1}. These changes tend to offset each other in the calculation of the conditional exceedance rate. However, near and above the unlimited-damper design limit tail load, $N(F_t|\sigma_{v_g})$ is much more sensitive to changes in $\bar{A}$, and the net effect *at 40 ft/s rms* is a 23% increase in $N(F_t|\sigma_{v_g})$ over the unlimited damper value of 0.0460 s^{-1}. Thus, for a 3.6 deg rudder limit, a small increase in the *overall* rate of exceedance of 46,511 lb is predicted.

A much larger increase would be predicted if the limit were halved to 1.8 deg. Gust velocity scales directly with authority limit for given values of $\bar{A}$ and N_0. Thus, to apply the Fig. 1 curves to the 1.8 deg limit, the abscissa gust velocities in Fig. 1 are halved. Gust velocities of 20 to 40 ft/s rms then correspond to values of $\bar{A}$ and N_0 substantially different from those for the unlimited damper. At $\hat{\sigma}_{v_g}$, these values are 657 lb-s/ft and 0.375 s^{-1}, respectively, yielding more than a threefold increase in the conditional exceedance rate at this σ_{v_g} over the value for the unlimited yaw damper. This limit was therefore also analyzed, since the system was not very nonlinear at the higher limit over the tail load range of interest.

The Eq. (3) integrand for the 1.8 deg limit is included in Fig. 2 to demonstrate how well it scales relative to the unlimited damper integrand. Note the virtual coincidence of the peak values. Thus the increase in $N(F_t|\hat{\sigma}_{v_g})$ provides a good estimate of the increase in overall exceedance rate for this limit.

Design Limit Load

Figure 3 gives the overall exceedance rates as a function of tail load for the yaw damper with no authority limit and with the 3.6 deg and 1.8 deg limits. The exceedance rate curve for the unaugmented system is also included, providing an upper bound for damper limiting effects. The figure verifies the predicted increases in the rate of exceedance of 46,511 lb for the two finite-limit cases, and indicates further divergence of these curves from the unlimited damper curve with increasing tail load. This divergence is also predictable as a function of $\hat{\sigma}_{v_g}$ which, as noted, increases directly as the square root of tail load. In terms of mission analysis design limit tail load, Fig. 3 shows that:

1) Damper limiting can have a very large effect on the design limit load level, as indicated by the gap between the "damper-off" and "no-limiting" curves. This is, of course, the result of the marginally stable dutch roll characteristics of the unaugmented aircraft.

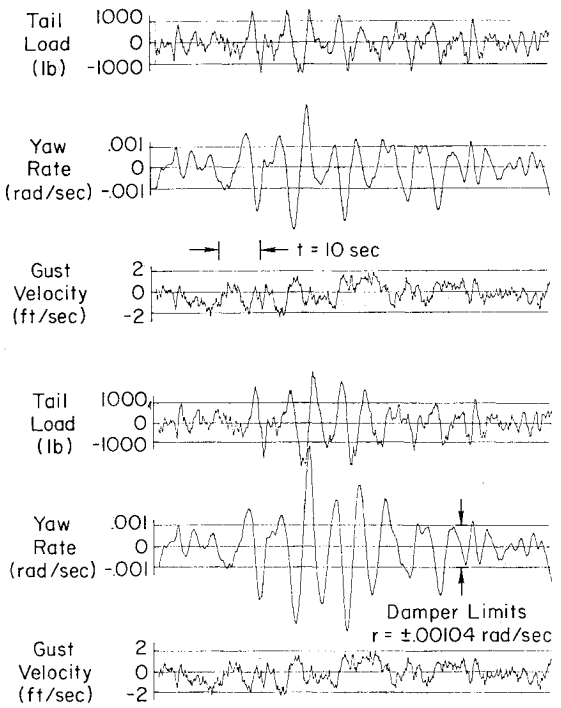

Fig. 5 Sample Monte Carlo simulation time histories: a) No limiting: $k_{DF} = 1.0$; b) Limiting: $k_{DF} = 0.6$.

2) At approximately the limit used on the 747 there is a negligible increase in limit load. However, halving this limit increases design limit load by 20%.

Time Domain Simulation

Description

A digital simulation of the nonlinear system was used to measure exceedance rates of the tail load in the time domain. Time functions were calculated using a fixed-interval Runge-Kutta integration scheme. To match the gust velocity distributional and spectral characteristics required by the mission analysis, a normal distribution of zero mean and unit variance was pseudo-randomly sampled and the result was appropriately scaled for a given rms level and filtered. The simulation then amounted to a Monte Carlo analysis in which the tail load was treated as a random process for which we wished to measure exceedance rates.

A run length of 30 min was selected to provide a reasonable tradeoff between the cost of running the simulation and the accuracy of the measurements. Based on the assumption that at least five exceedances are needed for reasonable accuracy, this time duration allows estimation of exceedance rates as low as 0.0014/s if the exceedances for positive and negative values of tail load are pooled. For the linear no-limiting case, this rate occurs at roughly the 3σ level of F_t for any given σ_{v_g}. To extend the region of accuracy to the 4σ level would require roughly 30 times this run length, or 15 h (see Fig. 4). Since the data generated for a given rms gust velocity and authority limit can readily be scaled to apply to any combination with the same ratio of gust velocity and authority limit, an rms gust velocity of 1 ft/s was arbitrarily chosen as the input for all Monte Carlo runs.

Validation

The simulation was validated by making a run with no damper limit ($k_{DF} = 1$). The probability distribution and exceedance rates obtained from the simulation are compared with the analytical solution in Fig. 4. Figure 4a shows that the tail load is indeed normally distributed. The data match the theoretical curve extremely well. Likewise, Fig. 4b shows a very good match of the exceedance rates to at least as low as 0.003/s with accuracy to within 20% and generally better than 10%, and close agreement between $\pm F_t$ exceedances. Below 0.003/s the number of exceedances is too small to provide an accurate estimate of the rates. Nonlinear simulation runs were made at authority limits corresponding to describing function effective gains (k_{DF}) of 0.8, 0.6, and 0.2.

Figure 5 compares sample time histories of tail load, yaw rate, and gust velocity for the unlimited yaw damper with a corresponding segment from the run at $k_{DF} = 0.6$. Identical gust velocity inputs provide a time reference for comparison of the system responses. The segment chosen for comparison features a very turbulent patch sandwiched between two lulls. It was selected to demonstrate the effects of the rudder authority limit. Comparison of the traces shows that: 1) during the lulls, when yaw rate remains within the authority-limit band for an extended period of time, differences in the tail forces traces are negligible, and 2) during the turbulence patch which is marked by large rapid changes in gust velocity, the yaw rate frequently exceeds the limited damper authority, producing very substantial increases in tail load.

Results

Comparison with Describing Function Analysis

Conditional exceedance rates for the three nonlinear runs are compared with those computed using the $\bar{A}$ and N_0 values determined by describing function analysis in Fig. 6. As the damper limit is reduced ($k_{DF} = 0.8$) the exceedance rates given by describing function for large tail loads begin to depart from the simulation-based curves. The differences are greatest at $k_{DF} = 0.6$. As the authority limit goes to zero ($k_{DF} = 0.2$) the tail load characteristics approach those of the airplane without a yaw damper. This system behavior becomes more linear and describing function results approach those obtained from the time domain simulation.

These results clearly show that describing function analysis can substantially underestimate the exceedance rates for large tail loads when damper operation becomes highly nonlinear. Moreover, for the case where the describing function is at least accurate ($k_{DF} = 0.6$), the analytical empirical difference appears to be diverging with increasing load except for the last and least accurate Monte Carlo data point at 2500 lb. Unfortunately, the data are too limited to permit a firm conclusion to be drawn on this point.

These conditional exceedance rate data were used to compute overall exceedance rates for comparison with those determined by describing function analysis. As in that approach, this computation is based on Eq. (3). In the Monte Carlo case, however, the value of $N(F_t | \sigma_{v_g})$ is not analytically expressible. Instead this value was interpolated directly from the tabulated simulation results.

Overall exceedance rates thus determined are compared with the describing function results in Fig. 7. This comparison indicates that:

1) For the 3.6 deg rudder limit, describing function analysis adequately predicts limit load exceedance rates. However, linear analysis of the damper with no authority limit does almost as well because the effect of the nonlinearity is not important at the design limit load. At increasing tail loads describing function analysis becomes more unconservative, though the differences are rather small.

2) Halving the authority limit to 1.8 deg substantially decreases the accuracy of the describing function analysis. The Monte Carlo results indicate a 27% increase in the limit load from the value for the unlimited yaw damper, compared with the 20% increase previously noted for describing function analysis. The Monte Carlo data also indicate that the latter approach underestimates exceedance rates for 60,000 to 80,000 lb by roughly a factor of 2.

Clearly, describing function analysis cannot be counted on to give a conservative estimate of design limit load.

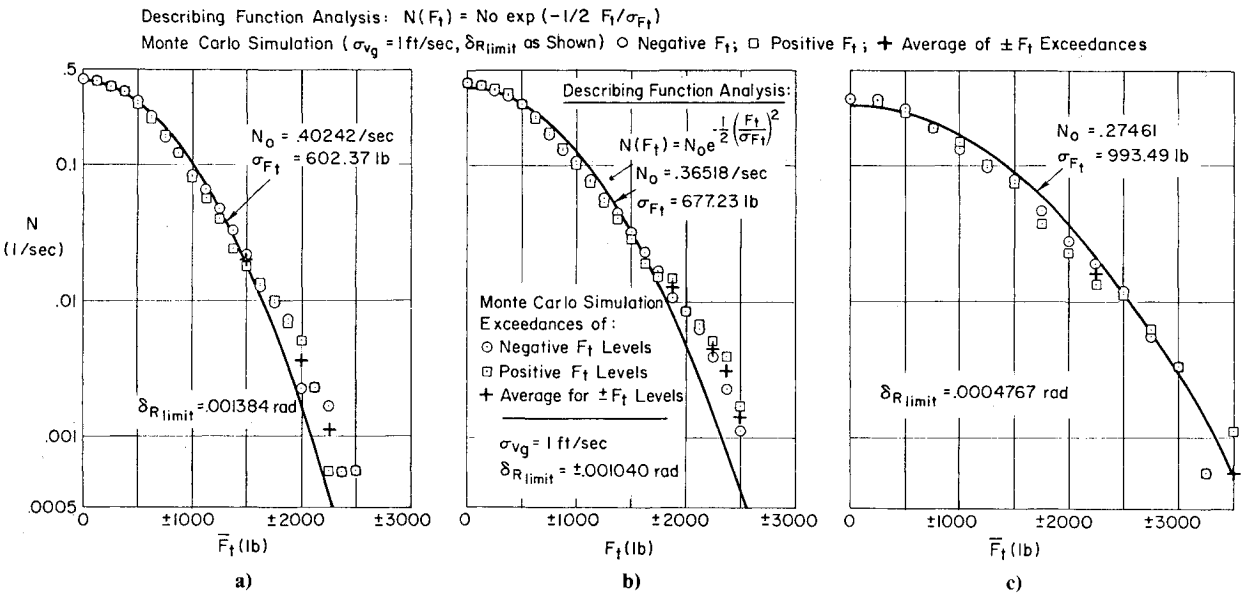

Fig. 6 Comparison of conditional exceedance rates for time domain simulation with describing function analysis results. a) $k_{DF} = 0.8$; b) $k_{DF} = 0.6$; c) $k_{DF} = 0.2$.

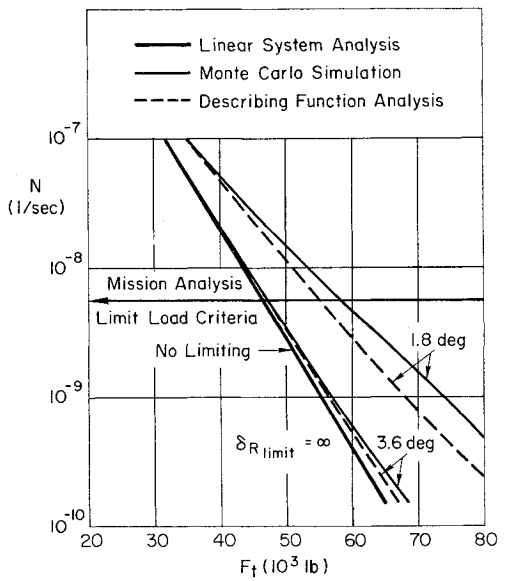

Fig. 7 Overall exceedance rates from describing function analysis vs time domain simulation.

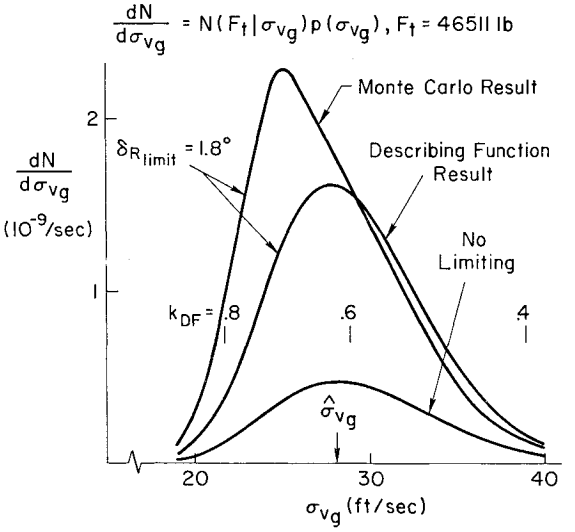

Fig. 8 Comparison of variation of overall exceedance rate integrand.

Application of Critical Gust Velocity Concept

As with the linear (no limiting) and describing function results, differences between describing function and Monte Carlo overall results can be predicted from conditional exceedance rate data, though with considerably greater difficulty and less precision. Because a quantitative prediction could not be readily made in this case, it was not discussed previously. It is discussed here because the predictive process can be used to indicate the adequacy of describing function analysis.

The prediction focuses once again on the no-limiting design limit load. At the corresponding critical velocity previously determined (28.2 ft/s), and a rudder limit of 3.6 deg, the describing function gain k_{DF} is 0.98. Therefore, system behavior is nearly linear and either describing function or linear analysis is adequate. For a rudder limit of 1.8 deg, k_{DF} is very close to 0.6. Thus conditional exceedance rates shown in Fig. 6b apply, if F_t is scaled by $\hat{\sigma}_{v_g}$. At the scaled value of the design limit load, 1650 lb (46,511/28.2), differences between the describing function and Monte Carlo results are negligible. However, coincidence at this point cannot be interpreted as validating the describing function analysis.

Examination of the entire range of scaled tail loads in Fig. 6b shows that the describing function results are not very accurate at other gust levels near $\hat{\sigma}_{v_g}$. The largest discrepancies occur at higher loads, or lower gust levels, where the Monte Carlo exceedance rates are considerably greater. The higher overall exceedance rates, and thus the higher design limit load, from the Monte Carlo analysis are therefore to be expected.

The Monte Carlo/describing function differences are shown clearly in Fig. 8. The differences at the gust intensities below $\hat{\sigma}_{v_g}$ are obviously considerably more significant than the ones at higher gust levels. Furthermore, the magnitude of the difference could not be estimated by checking only one gust level. The two curves differ in shape and size.

The above discussion does not negate the importance of the $\hat{\sigma}_{v_g}$ gust level. It can still be used to evaluate a describing function analysis. Comparison of Monte Carlo and describing function exceedance rates for that gust level will still indicate the validity of the describing function analysis; however, the comparison must include a broad range of loads about the design limit load.

Summary

The effect of a simple, and common, control system nonlinearity on mission analysis calculations of design limit loads has been examined for a realistic aircraft design problem. Random input describing function analysis was used to approximate the effect of the nonlinear element. This allowed direct carryover of the standard power spectral techniques used for linear system analysis; however, the computations had to be repeated for various rms gust velocity levels, to define variations of $\bar{A}$ and N_0 with gust level.

Through comparison with results obtained from a time domain simulation of the nonlinear system, it was shown that, for the case in point, the describing function approach tends to underestimate the frequency of large loads. For some levels of nonlinearity, it may provide a considerably unconservative estimate of design limit load. The basic problem is that describing function analysis can only approximate the loads as a normally distributed random process. Within that constraint the describing function approach does a good job. However, as shown by the simulation, the loads in this case were not well represented by a normal distribution at gust levels at which system behavior was highly nonlinear.

It would be difficult to extrapolate this result directly to other situations involving, for example, different and/or multiple nonlinearities. On the other hand, the routine use of a time domain simulation to establish design limit loads in every situation involving system nonlinearities is not an attractive alternative. A Monte Carlo analysis of such rare events as exceedances of design loads would be very costly, especially for large aircraft which require the inclusion of structural modes.

Critical Gust Velocity Concept

While the results for the example problem are not directly applicable to the general case, the analysis presented here serves to illustrate a cost-effective compromise approach. The key to this approach lies in the selection of the appopriate gust intensities. As was shown for the example, the gust velocity which causes the greatest increment to the overall exceedance rate is easily determined for the linear system. It was also demonstrated that nonlinear effects do not change this critical gust velocity drastically; it is largely determined by the gust probability distribution and the load level of interest. The analysis also suggests a simple way of using this fact to minimize the costs of nonlinear analysis.

As noted, a critical gust level can be identified from the conventional linear analysis results. A describing function analysis for that gust level will indicate if the nonlinear effects are significant. If they are, a Monte Carlo simulation can be run at the critical gust level to determine the adequacy of the describing function analysis. The concept of a critical gust level is important because of the drastic cost increase in going from linear analysis to describing function analysis to Monte Carlo simulation. This concept provides a method for determining when either of the cheaper methods (linear or describing function analysis) is adequate.

Appendix

Mission Analysis Criteria Derivation

First, it is assumed that each patch of turbulence can be adequately modeled as a normally distributed random process with a standard deviation σ_g. The gust intensity σ_g is in turn modeled as a random variable with a probability density function $p(\sigma_g)$. Then for any one flight segment the exceedance rate is given by:

$$N(\Delta x) = \int_0^\infty N(\Delta x | \sigma_g) p(\sigma_g) \, d\sigma_g \tag{A1}$$

where $N(\Delta x | \sigma_g)$ is the exceedance rate for Δx when the gust intensity is σ_g. For a linear system excited by a normally distributed random process, the exceedance rate is:

$$N(\Delta x | \sigma_g) = N_0 \exp\left[-\frac{1}{2} \left(\frac{\Delta x}{\bar{A}\sigma_g} \right)^2 \right] \tag{A2}$$

where $\bar{A}\sigma_g = \sigma_x$ and N_0 is the upward axis crossing rate, given by $(1/2\pi)\ (\sigma_{\dot{x}}/\sigma_x)$, the radius of gyration, in Hz, of Δx power spectral density about zero frequency.

For the intensity probability density function it is assumed that there are two kinds of turbulence, nonstorm and storm. The probabilities of encountering each are P_1 and P_2, respectively (probability of no turbulence is $1 - P_1 - P_2$). Given that turbulence has been encountered, the intensity σ_g is assumed to have a normal distribution with an rms value of b_1 or b_2. Thus, the probability density function for turbulence intensity can be written as:

$$p(\sigma_g) = \sqrt{\frac{2}{\pi}} \left\{ \frac{P_1}{b_1} \exp\left[-\frac{1}{2} \left(\frac{\sigma_g}{b_1} \right)^2 \right] + \frac{P_2}{b_2} \exp\left[-\frac{1}{2} \left(\frac{\sigma_g}{b_2} \right)^2 \right] \right\} \tag{A3}$$

The final design equation, Eq. (1) is obtained by: 1) combining Eqs. (A1, A2, A3); 2) using the definite integral

$$\int_0^\infty \exp\left(-y^2 - \frac{a^2}{y^2} \right) dy = \frac{\sqrt{\pi}}{2} e^{-2|a|}$$

and 3) weighting the exceedance rates for each mission segment by the fraction of time spent in the segment and summing over all segments.

System Model

Equations (in Laplace Transform notation)

$$F_t = \frac{F_\beta \beta_t + F_\delta \delta_R}{\tau s + 1} \qquad sr = -\frac{F_t l_t}{I_z}$$

$$\beta_t = \beta - \frac{v_g}{V} - \frac{l_t r}{V} \qquad \delta_R = K_R r \leq \delta_{R_{\text{limit}}}$$

$$s\beta = -r + \frac{F_t}{mV} \qquad \phi_{v_g}(\omega) = \frac{2\omega_g}{\pi} \frac{\sigma_{v_g}^2}{\omega^2 + \omega_g^2}$$

Describing Function Analysis

Based on the assumption that both input and output are ergodic random processes, the random input describing function for a simple, isolated nonlinearity is derived by Graham and McRuer[8] as:

$$k_{DF} = \frac{\int_{-\infty}^{\infty} x f(x) p(x) \, dx}{\int_{-\infty}^{\infty} x^2 p(x) \, dx}$$

where x is the input to the nonlinear element, $p(x)$ is its probability density, and $f(x)$ is the output of the nonlinear element.

For a simple limiter with unit slope and limits of $\pm a$, whose input has a Gaussian probability density, the result is:[8]

$$k_{DF} = \text{erf}\left(\frac{a}{\sqrt{2}\sigma_x} \right) \tag{A4}$$

The describing function analysis proceeds from this relationship, based on the assumption that the rudder deflection, as well as all other response variables, are well represented as normally distributed random variables, as they would actually be in the linear case. Expressing k_{DF} in terms

of the rudder deflection, reflected back to the limiter input, and the authority limit gives

$$k_{DF} = \text{erf}\left(\frac{\delta_{r_{\text{limit}}}}{\sqrt{2}(\sigma_{\delta_R}/k_{DF})} \right)$$

Thus the relationship between authority limit and the describing function gain can then be expressed explicitly, in terms of the system input σ_{v_g}, as:

$$\frac{\sigma_{v_g}}{\delta_{R_{\text{limit}}}} = \left(\frac{\sigma_{v_g}}{\sigma_{\delta_R}} \right)_{CL} \frac{k_{DF}}{\sqrt{2}\,\text{erf}^{-1}(k_{DF})}$$

where $(\sigma_{v_g}/\sigma_{\delta_R})_{CL}$ is the rms response ratio for the closed-loop system.

This expression cannot be solved for k_{DF}, given a known $\delta_{R_{\text{limit}}}$, since the closed-loop response ratio depends on k_{DF}. The solution for a given σ_{v_g} and $\delta_{R_{\text{limit}}}$ can only be obtained by iterative evaluation for various values of k_{DF}. The first step in each case is to compute the system transfer functions with the yaw damper loop closed for a selected value of k_{DF}. The rms gust velocity responses are then calculated using the standard formula:

$$\sigma_x = \left(\int_0^\infty \left| \frac{x}{v_g}(j\omega) \right|^2 \phi_{v_g}(\omega)\,d\omega \right)^{1/2}$$

These responses can, in turn be used to compute other basic parameters, e.g., $\sigma_{v_g}/\delta_{R_{\text{limit}}}$, $\sigma_{\dot{F}_t}/\sigma_{F_t}$.

Acknowledgment

This work was supported by the Systems Research Development Service of the FAA under Contract DOT-FA77WA-3936 with E. M. Boothe as Contract Technical Monitor.

References

[1] "(Proposed) Appendix G, Continuous Gust Design Criteria, FAR Part 25—Airworthiness Standards: Transport Category Airplanes," *Federal Register*, Vol. 40, No. 112, Tuesday, June 10, 1975, pp. 24812-24813.

[2] Hoblit, Frederic M., "Effect of Yaw Damper on Lateral Gust Loads in Design of the L-1011 Transport," *Active Control Systems for Load Alleviation, Flutter Suppression, and Ride Control*, AGARD-AG-175, March 1974.

[3] Sidwell, Kenneth, "A Method for the Analysis of Nonlinearities in Aircraft Dynamic Response to Atmospheric Turbulence," NASA TN D-8265, Nov, 1976.

[4] Stapleford, R.L. and DiMarco, R.J., "A Study of the Effects of Aircraft Dynamic Characteristics on Structural Loads Criteria," FAA-RD-78-155, Nov. 1978.

[5] Stauffer, W.A. and Hoblit, F.M., "Dynamic Gust, Landing, and Taxi Loads Determination in the Design of the L-1011," *Journal of Aircraft*, Vol. 10, Aug. 1973, pp. 459-467.

[6] Austin, W.H., "The Effects of Atmospheric Turbulence on Handling Qualities and Structural Loads," presented at Royal Aeronautical Society, International Conference Atmospheric Turbulence, London, England, May 1971.

[7] Heffley, R.K. and Jewell, W.F., "Aircraft Handling Qualities Data," NASA CR-2144, Dec. 1972.

[8] Graham, D. and McRuer, D., "Analysis of Nonlinear Control Systems," Dover, New York, 1971.